# COMBINED HYPERSPECTRAL AND FIELD MAPPING ALONG THE 1999 HECTOR MINE EARTHQUAKE SURFACE RUPTURE


Witkosky, R.[1,*], Akciz, S.[2], Buckland, K.[3], Harvey, J., Hudnut, K.[4], Kendrick, K.[4], Lynch, D.[3], Scharer, K.[4], Sousa, F.[1], Stock, J.[1], Tratt, D.[3]

[1]Caltech, [2]UCLA, [3]The Aerospace Corporation, [4]USGS


Poster #266


## I. Abstract

We explore the use of infrared hyperspectral remote sensing techniques combined with field observations to perform geologic mapping along the 1999 Hector Mine earthquake surface rupture. Existing geologic maps of this region are based on field studies completed more than four decades ago. Field access to the location of the surface rupture is highly restricted, but in April 2014 we were granted limited access to collect geologic ground-truth data. We mapped a ~4500 $m^2$ area of well-exposed volcanic bedrock, digitized and georeferenced the geological unit contacts from this map, and compared this to a swath of hyperspectral data from Mako, an airborne spectrometer built by The Aerospace Corporation. The Mako airborne imagery provides 2-m pixel resolution along a 1.8 km-wide swath centered on the Lavic Lake fault, the site of 1999 earthquake maximum slip zone. Mako captures 128 bands in the thermal infrared covering 7.8 to 13.4 microns. Mako's high spatial and spectral resolution, along with the lack of a significant vegetation cover in the study area, makes it possible to distinguish distinct small bedrock outcrops and geomorphic surfaces proximal to the fault. With the geologic unit contacts superimposed on the hyperspectral imagery, pixels with ground-truthed lithology were chosen from the Mako data to train a supervised classification of the same ~4500 $m^2$ area. The resulting map from the supervised classification was then compared with the ground-truthed field map to assess the user accuracy of a remotely-produced product. Preliminary results show that for a small area, a Mako-based geologic map can be produced with a user accuracy of ~50%, based on an error matrix. Further refinements to our technique will improve the data processing sequence and increase the signal-to-noise ratio. These improvements will likely result in geologic maps that have a greater areal extent and higher user accuracy, and should be useful for initial mapping in restricted areas or remote terrain.


## II. Introduction & Overview of the Study Area

Figure 1 Map of the study area: Mojave Desert, eastern California, including the 48 km dextral surface rupture along the Lavic Lake and Bullion faults created by the 1999 Hector Mine earthquake (faults are from U.S Geological Survey and California Geological Survey, 2006). Red boxes outline north and south Mako data sets. Total data coverage is 1.8 km wide by 11 km long. Data covers the maximum slip zone (>5 m dextral slip) from Treiman et al. (2002).

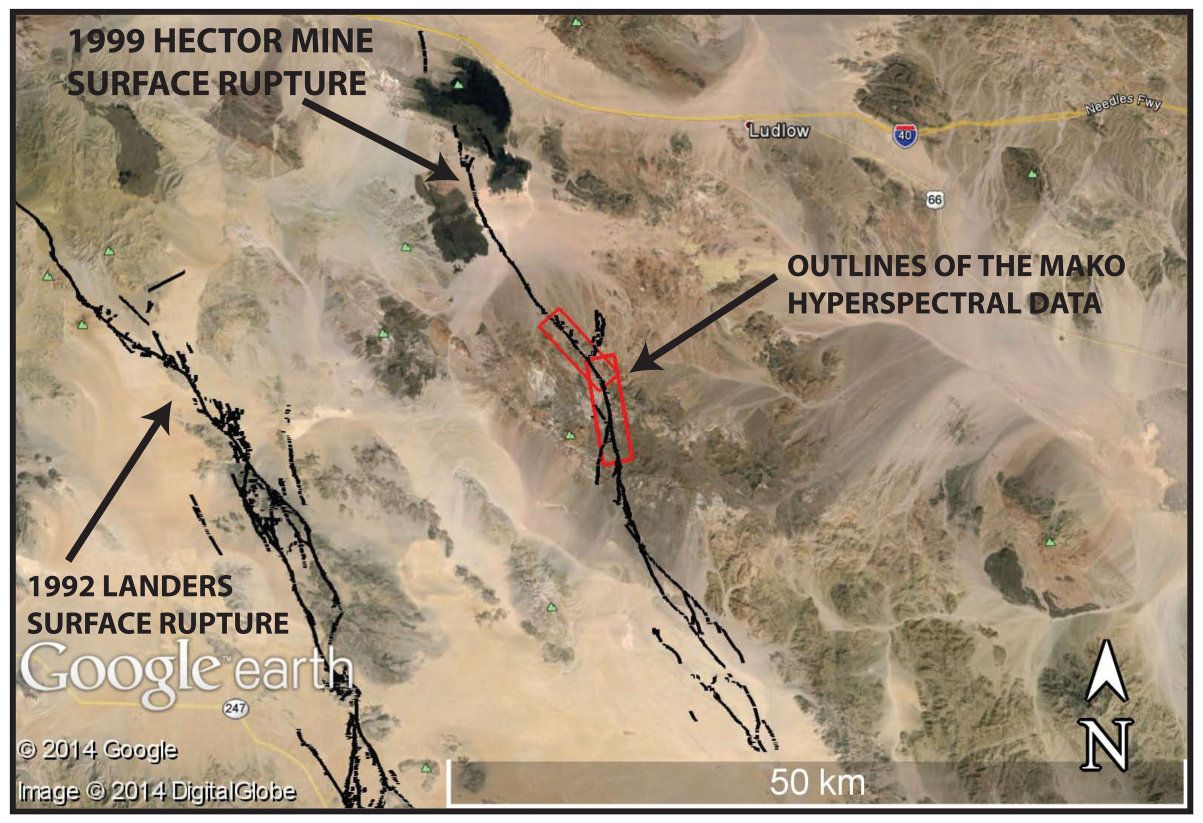


Figure 2 Map by the Aerospace Corporation showing north Mako data set (from Figure 1) georeferenced and superimposed on to NAIP (National Agriculture Imagery Program) aerial imagery. Variation in color represents differences in lithology.

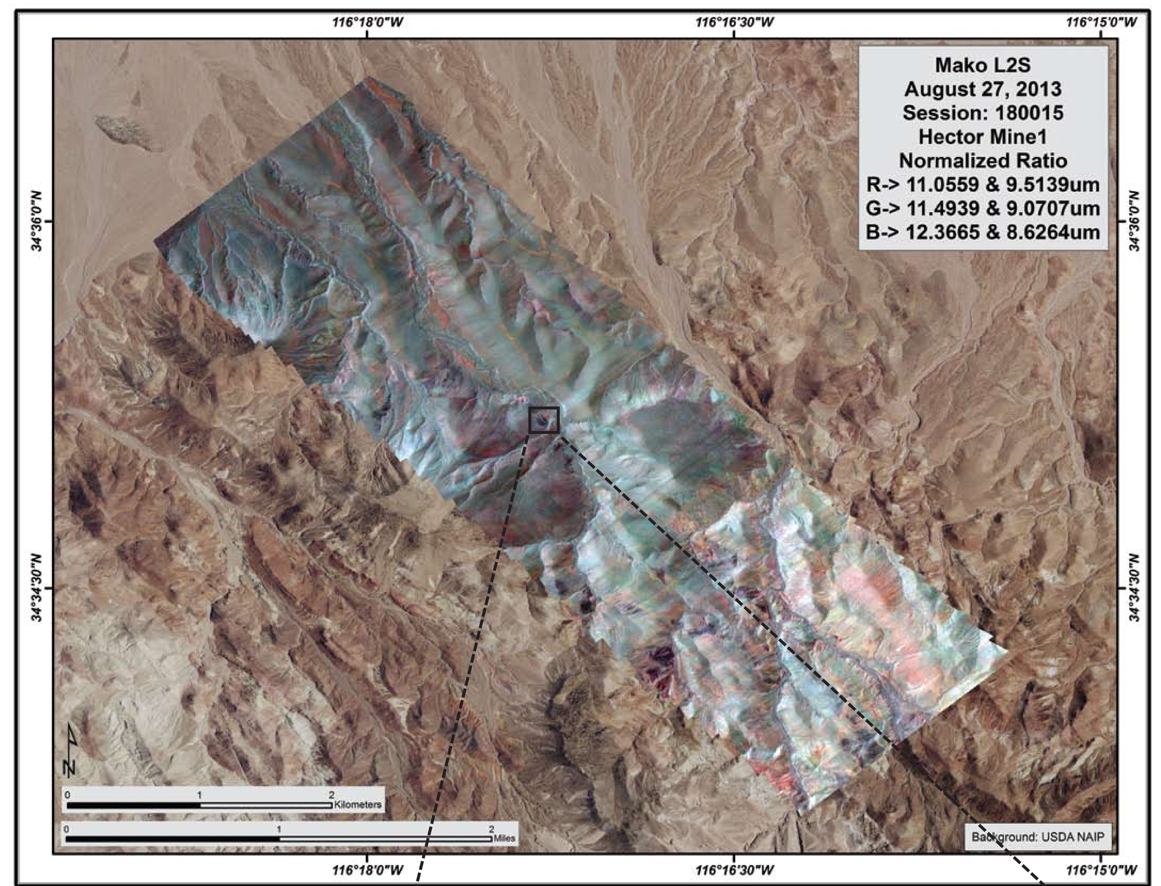


## III. 2014 Field Work

Figure 3 2014 Field work included geologic mapping and many other activities: 1- J. Harvey collecting samples; 2- K. Scharer mapping gullies offset by the 1999 surface rupture using GPS; S. Akciz and R. Witkosky measuring the offset; 3- F. Sousa and K. Scharer measuring a ridge offset by the surface rupture (**SEE SOUSA ET AL., THIS SESSION, POSTER #258**); 4- K. Scharer studying the Red Flake, an outcrop of volcanic rock along the surface rupture; 5- K. Hudnut collecting terrestrial LiDAR data along the fault scarp; 6- selfie of the field working group (S. Akciz, K. Scharer, F. Sousa, R. Witkosky, K. Hudnut, J. Stock, J. Harvey, and D. Lynch, clockwise from left); 7- R. Witkosky; 8- Red Flake (fault runs down the center of the image). Photo credit to J. Stock for #'s 1,2,3,4,5 & 8, and to Dave Lynch for #'s 6 & 7.


Figure 4 Red Flake Site: white lines are lithologic contacts, black lines are the 1999 surface rupture mapped by Treiman et al. (2002). The "Red Flake" is a prominent fault scarp composed of red feldspar porphyry (see also in Figures 3.4 & 3.8). This site serves as ground-truth to test how well the hyperspectral data can differentiate between distinct lithology on a very fine scale (tens-of-meters).

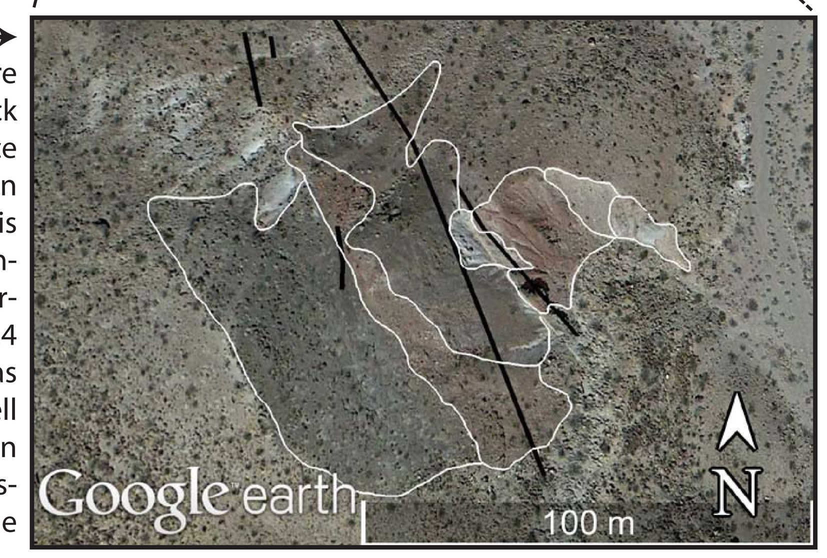


## IV. Hyperspectral Data Processing*

START: Level 2 data cubes delivered by the Aerospace Corporation

→ Create band ratios → Georeference → Superimpose faults and lithologic contacts → END: Figure 5

→ ISAC (In-Scene Atmospheric Correction) → Calculate temperature and emissivity using the emissivity normalization algorithm (Kealy and Hook, 1993) → Supervised Classification → Georeference → Superimpose faults and lithologic contacts → END: Figure 6-1

ISAC Parameters:
Regression Pixels = Max Hit
Fitting Technique = Normalized Regression
NESR (Noise Equivalent Spectral Radiance) = 0.7

Emissivity normalization Parameter:
Assumed Emissivity Value = 0.97

Supervised Classification Method: SAM (Spectral Angle Mapper) algorithm
Maximum angle (single value, radians) = 0.1

*All processing done using ENVI (ENvironment for Visualizing Images) Software

Figure 5 Band ratio image of the Red Flake Site from Mako hyperspectral data. Band ratios are the same as shown in Figure 2. White lines are lithologic contacts, and black lines are the 1999 surface rupture, superimposed from Figure 4.

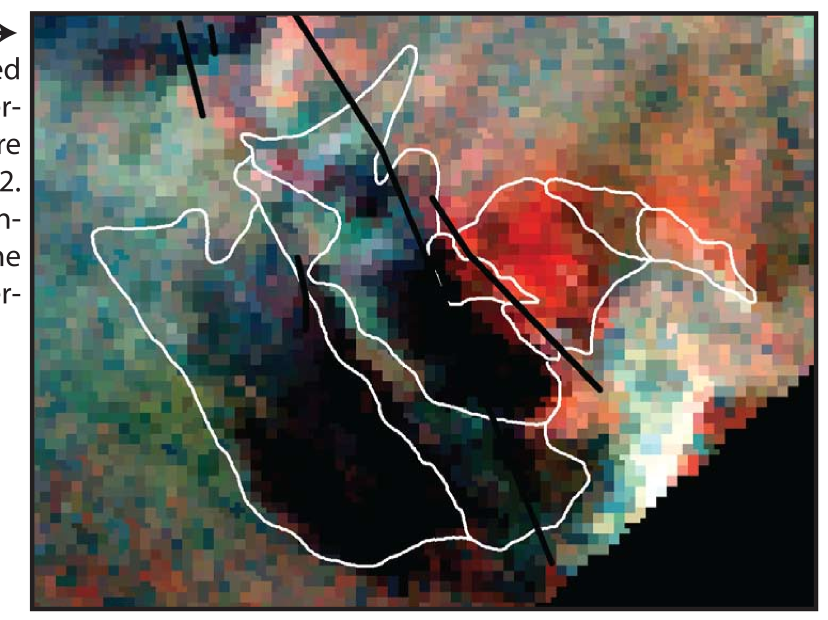

## V. Supervised Classification of the Red Flake Site

Figure 6 1- Supervised Classification of the Red Flake Site; and 2- idealized map showing 100% accuracy. For 1, a few training pixels are selected from each region, and pixels with a similar spectrum (within a specified threshold) are identified throughout the scene. The SAM algorithm uses the dot product to calculate the n-dimensional (n = number of bands) angle between each pixel and the training pixels (smallest angle within the threshold wins).

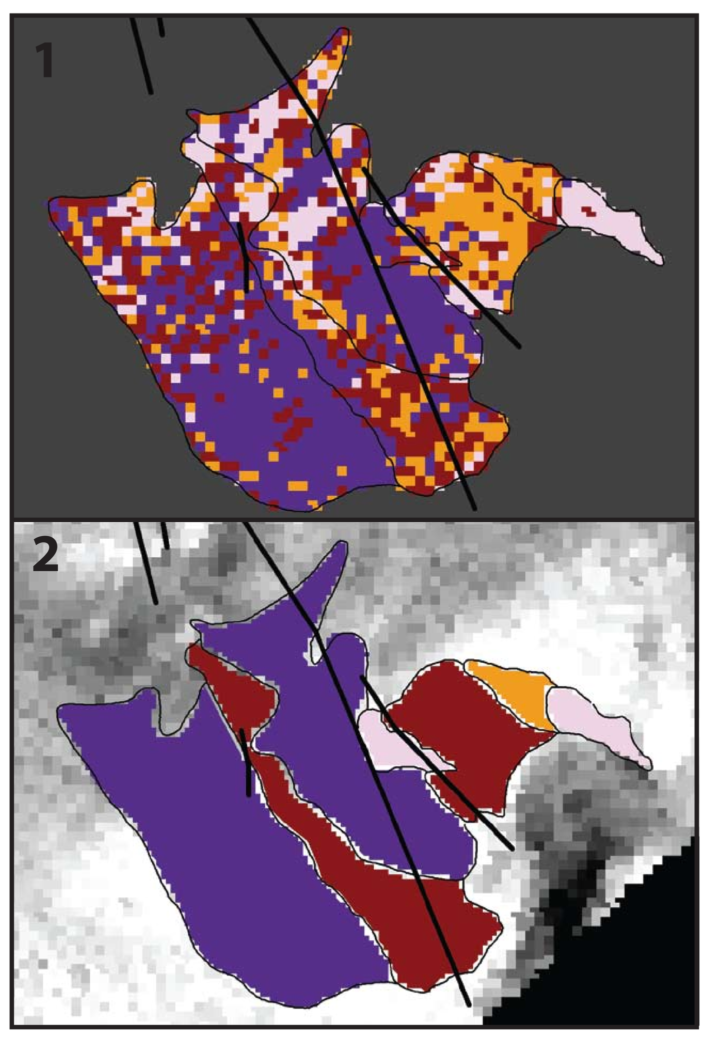


**LEGEND**

- Tuff (and tuff breccia)
- Detritus (sand and gravel)
- Feldspar porphyry
- Basaltic andesite

Figure 7 A- Error matrix for the supervised classification displays the number of pixels misidentified in each ground-truthed area, and what they were misidentified as.
B- Statistics for the error matrix. Omissions are for a given row, the sum of the error pixels divided by row total, and commissions are similar, but for a given column. User's accuracy depicts the percentage of pixels that, in reality, are what the map calls them (Congalton, 1991).

**Accuracy Assessment of the Red Flake Site: Supervised Classification in ENVI using the Spectral Angle Mapper (SAM) Algorithm**

**A**

| Ground Truth Families | ENVI Classes | | | | |
|---|---|---|---|---|---|
| | Tuff | Detritus | Feldspar Porphyry | Basaltic Andesite | Row Total |
| Tuff | 137 | 24 | 23 | 61 | 245 |
| Detritus | 19 | 67 | 30 | 1 | 117 |
| Feldspar Porphyry | 214 | 472 | 495 | 267 | 1448 |
| Basaltic Andesite | 395 | 395 | 698 | 1881 | 3369 |
| Column Total | 765 | 958 | 1246 | 2210 | 5179 |

**B**

| | Number of Pixels (2 $m^2$ pixels) | Area ($m^2$) | Commissions | Omissions | Producer's Accuracy | User's Accuracy |
|---|---|---|---|---|---|---|
| Tuff | 54 | 216 | 82% | 44% | 56% | 18% |
| Detritus | 72 | 288 | 93% | 43% | 57% | 7% |
| Feldspar Porphyry | 282 | 1128 | 60% | 66% | 34% | 40% |
| Basaltic Andesite | 731 | 2924 | 15% | 44% | 56% | 85% |
| OVERALL ACURACY = 50% | | | | | | |

## VI. Summary and Future Work

- A variety of volcanic lithology is found along the fault zone, along with detrital geomorphic surfaces.

- In the supervised classification, homogeneous lithology (basaltic andesite) yields the highest user accuracy, but heterogeneous lithology (detritus) confuses the classification algorithm, leading to a very low user accuracy.

- Using a combination of field knowledge, band ratio maps and supervised classifications, this study can be extended to produce a geologic map covering the entire 11 km swath of Mako data.

- A complete map could highlight offset volcanic bedrock or geomorphic surfaces, which would help to target specific sites for future field work.


*contact: rampryan@caltech.edu



## VII. Acknowledgements

This work is funded by SCEC Award Number 14160. Thank you, SCEC! We also acknowledge the MCAGCC (Marine Corps Air Ground Combat Center) in Twenty Nine Palms, California, for allowing us access to the military base to study the geology of the region. Mako airborne hyperspectral imagery was acquired under the auspices of the Aerospace Corporation's Independent Research and Development program.


## VIII. References


Congalton, R. G. (1991). A review of assessing the accuracy of classifications of remotely sensed data, Remote Sens. Environ. 37, 35-46.

Kealy, P. S., and S. J. Hook (1993). Separating temperature and emissivity in thermal infrared multispectral scanner data: Implications for recovering land surface temperatures, IEEE Transactions on Geoscience and Remote Sensing Vol. 31, No. 6, 1155-1164.

Treiman, J. A., K. J. Kendrick, W. A. Bryant, T. K. Rockwell, and S. F. McGill (2002). Primary surface rupture associated with the Mw 7.1 16 October 1999 Hector Mine earthquake, San Bernardino County, California, Bull. Seism. Soc. Am. 92, 1171-1191.

U.S. Geological Survey and California Geological Survey, 2006, Quaternary fault and fold database for the United States, accessed 09/01/2014, from USGS web site: http//earthquakes.usgs.gov/regional/qfaults/.


***RESPONDING TO A DYNAMIC WORLD . . .***